Formation of Liesegang patterns: Simulations using a kinetic Ising model

T. Antal and M. Droz
Département de Physique Théorique, Université de Genève, CH 1211 Genève 4, Switzerland

J. Magnin
Département de Physique Théorique, Université de Genève, CH 1211 Genève 4, Switzerland and Center for Stochastic Processes in Science and Engineering and Department of Physics, Virginia Tech, Blacksburg, Virginia 24061-0435

A. Pekalski
Instytut Fizyki Teoretycznej, Uniwersytet Wrocławski, Wroclaw, pl. M. Borna 9, 50-204 Wroclaw, Poland

Z. Rácz
Institute for Theoretical Physics, Eötvös University, 1117 Budapest, Pázmány sétány 1/a, Hungary

(Received 3 October 2000; accepted 30 November 2000)

A kinetic Ising model description of Liesegang phenomena is studied using Monte Carlo simulations. The model takes into account thermal fluctuations, contains noise in the chemical reactions, and its control parameters are experimentally accessible. We find that noisy, irregular precipitation takes place in dimension $d=2$ while, depending on the values of the control parameters, either irregular patterns or precipitation bands satisfying the regular spacing law emerge in $d=3$. © *2001 American Institute of Physics.* [DOI: 10.1063/1.1342858]

I. INTRODUCTION

Quasiperiodic precipitation patterns emerging in the wake of chemical reaction fronts are called Liesegang patterns.[1,2] They have been studied for more than a century and a number of theoretical approaches have been developed to explain the experimental observations.[3] Nevertheless, it was only recently that a model with input parameters fewer than the number of static and dynamic parameters characterizing the patterns has appeared.[4]

This last theory is based on the assumption that the main ingredients of a macroscopic description should be a moving reaction front and the phase separation of the reaction product behind the front. Taking the properties of the reaction front from the theory of the fronts in the $A+B\rightarrow C$ process[5] and describing the phase separation process by the Cahn–Hilliard equation,[6] one arrives at a model with a minimal number of parameters.

The above theory successfully explains that the positions x_n of the precipitation bands form a geometric series, $x_n \sim (1+p)^n$ (spacing law [7]), and gives the spacing coefficient p in terms of the initial concentrations of the reactants A and B in agreement with the Matalon–Packter Law.[8,9] Furthermore, the parameters in the model can be determined from experiments and the time scale of the emergence of a band can be calculated.[10] Finally, the width law relating the position and the width of the bands can also be derived[10,11] in agreement with observations.[12]

The success and versatility notwithstanding, this theory needs further developments since, in its present form,[4] it is a mean field theory without the fluctuations being accounted for. There are two ways to include the fluctuations. One is to add conserved thermal noise to the Cahn–Hilliard equation as it is done in Model B of critical dynamics.[13] In this case, there would be an additional problem of handling the noise in the reaction zone. It has been shown,[14] however, that this noise is irrelevant for $d>2$ so, in principle, it could be neglected.

In this work, another approach is taken for including the fluctuations. Namely, we shall study the kinetic Ising model version of the process and thus include the noise through the probabilistic description of the transitions between discrete states of the system.

There are several reasons for our choice. First, the problem of difference between the handling of fluctuations in the diffusive and reaction processes does not arise. Second, the kinetic Ising version of the model has a meaning of a mesoscopic (or perhaps a microscopic) description. Since the mechanism of band formation may be at work at a length-scale that makes possible the construction of submicron Liesegang structures, this kinetic Ising model approach may have a direct bearing on future experiments.[15] Third, our choice was also influenced by having more expertise in simulations of kinetic Ising models.

We shall start (Sec. II) by a detailed discussion of the kinetic Ising model designed to describe the band formation. The simulation results for this model are presented in Sec. III. First, the $d=2$ case is treated where we do not find regular band formation. Then the $d=3$ simulations are discussed which show the emergence of Liesegang patterns satisfying the usual spacing law. A summary, suggestions for experiments, and comments about a possible comparison of the parameters in the Cahn–Hilliard and the kinetic Ising model description can be found in Sec. IV.

II. KINETIC ISING MODEL DESCRIPTION

A. General aspects of the theory

The aim of the theories of Liesegang phenomena is to explain how a high-concentration electrolyte A diffuses into

a gel soaked by a low-concentration electrolyte B and how the spatial distribution of the precipitate D is formed in the wake of the diffusive reaction front. Accordingly, all the theories follow the scheme

$$A+B\rightarrow C\rightarrow D, \tag{1}$$

where C is an intermediate reaction product which is generally not very well known. This uncertainty is then the basis for the existence of a number of competing theories[16–23] with the differences arising from the interpretation of C and from the level of details in the description of the dynamics of C's. A significant drawback of all these theories is that they contain a large number of parameters and many of them are uncontrollable experimentally. Thus it is not entirely surprising that thorough comparisons between experiments and theories have not been carried out.

B. Cahn–Hilliard equation with source

In our view, the uncertainty about the intermediate product and its dynamics can be used to advantage in building a general theory of band formation. One can interpret the concentration of C's, c, as a kind of *order parameter* that takes a value c_p in the ordered (precipitate) phase and another value c_g in the disordered (low-density) phase. The C's are obtained from the $A+B\rightarrow C$ process so they are produced in the reaction zone. Furthermore, the dynamics of C's obeys global conservation and it should be a phase-separation type dynamics since, in the expected final state, one has regions of high-(precipitation) and low-density (interband) regions in equilibrium. This phase-separation dynamics can be described on a coarse-grained level by the Cahn–Hilliard equation[6] with the generation of C appearing as an additional source term. The resulting equation for the space- and time-dependent order-parameter density, $c(x,t)$ is given by[4]

$$\partial_t c=-\lambda\Delta\left[\frac{\delta f(c)}{\delta c}+\sigma\Delta c\right]+S(x,t). \tag{2}$$

Here λ is a kinetic coefficient, $f(c)$ is the Landau–Ginzburg free energy of the system which should have two equal minima at $c=c_p$ and $c=c_g$. The term $\sigma\Delta c$ with $\sigma>0$ provides stability against short-wavelength fluctuations, and finally $S(x,t)$ is the production rate of C's in the reaction-diffusion process $A+B\rightarrow C$. The properties of the source are known.[5,24,25] It is localized, its center, x_f, moves diffusively ($x_f=\sqrt{2D_f t}$), and it leaves behind a uniform concentration c_0 of C's.

The parameters λ and σ in Eq. (2) can be used to set the time-scale and length-scale, respectively, and the source, S, is completely specified by the initial densities (a_0,b_0) and diffusion constants $(D=D_a\approx D_b)$ of A and B.[5,24,25] Only the function $f(c)$ remains to be parameterized. One expects that the details of this function will not affect the overall properties of the pattern-formation process, the existence of two minima at c_p and c_g being the only important feature. Thus, assuming, e.g., a coexistence curve that is symmetric about $\overline{c}=(c_p+c_g)/2$, one can parametrize this function as $f(c)=-\epsilon(c-\overline{c})^2+\gamma(c-\overline{c})^4$. The scale of the concentration can be set by the parameter γ and ϵ remains a free parameter in the theory. Consequently, one has a theory which has only a single adjustable parameter apart from the parameters setting the scale of the length, time, and the concentration field.

As discussed in the Introduction, all the observed general features of Liesegang phenomena can be derived from the above theory,[4] including the time scale of the emergence of a single band and the length-scale for the width of the bands.[10,11] Actually, it is somewhat surprising that the mean-field level description in terms of Eq. (2) performs so well. The reason for this may lie in the experimental observation that the patterns are frozen (they do not evolve over time scales extending up to 30 years[2]) meaning that the dynamics takes place at a very low effective temperature, i.e., the noise is negligible.

The noise may indeed be negligible in the late stages of the formation of precipitation bands but the initial stages should be related to some instabilities and there the fluctuations should play a more prominent role. In particular, the mean-field description relies on a spinodal-decomposition instability (the moving front generates particles and pushes the concentration past the spinodal) and the possibility for the precipitation to take place through a nucleation-and-growth mechanism (where the fluctuations are important) is completely lost.

C. Kinetic Ising model with Kawasaki+Glauber dynamics

In order to include fluctuations in the Liesegang process, a kinetic Ising model will now be considered that is, we believe, a finite-temperature extension of the theory embodied in Eq. (2). The model introduced below can be viewed in two ways. Either it is a discretization scheme to Eq. (2) and then the description is on a mesoscopic level with $c(x,t)$ being the discretized concentration of the order parameter, C. Or, it can also be viewed as a simulation of the stochastic motion of C's which are now particles at microscopic scales (in this case the coarse graining has been carried out in time). In the following we shall use the latter ''particle'' language.

Let us begin the introduction of discretized description by identifying the particles C with the up-spins of an Ising model on a hypercubic lattice. Then the down-spin sites are empty places and the formation of precipitation bands is modeled by a combination of spin-flip and spin-exchange dynamics.[26] Namely, the initial state is prepared with all spins down (no C particles present) and the localized front flips the down spins (Glauber dynamics[27]) thus producing the C's. The flip rate $w_{\mathbf{r}}$ at site $\mathbf{r}$ is given by

$$w_{\mathbf{r}}=S(x,t)\tfrac{1}{2}(1-\sigma_{\mathbf{r}}), \tag{3}$$

where $\sigma_{\mathbf{r}}=\pm 1$ is the Ising spin at site $\mathbf{r}=(x,\mathbf{r}_\perp)$ with x being the coordinate in the direction of the motion of the reaction front while $\mathbf{r}_\perp$ representing the coordinates in the transverse direction (length is measured in units of the lattice spacing a). The factor $(1-\sigma_{\mathbf{r}})$ ensures that the front flips only down spins (the particles are produced in the front and the back reaction is negligible). Finally, $S(x,t)$ is a function describing the motion of the reaction front and the change of the reaction rate with time. The front is assumed to be ho-

mogeneous in the transverse direction and its actual shape, $S(x,t)$, can be taken from the solution and simulations of the $A+B\to C$ process.[5,28] Since the width of the reaction zone is small and it changes with time very slowly, for all practical purposes, the function $S(x,t)$ can be approximated by a constant within a small interval $[x_f-\Delta,\ x_f+\Delta]$ around the center of the reaction zone $x_f=\sqrt{2D_f t}$,

$$S(x,t)=\frac{A}{\sqrt{t}}\,\theta(x-x_f+\Delta)\,\theta(x_f+\Delta-x), \tag{4}$$

where $\theta(x)$ is the step function and the amplitude

$$A=\frac{\sqrt{2D_f}}{4\Delta}c_0 \tag{5}$$

is chosen such that the front leaves behind a constant (c_0) concentration of particles.[3,5]

Once the particles are created, they diffuse and interact. This part of the dynamics can be described by a spin exchange process (Kawasaki dynamics[29]). The rates of the exchanges are assumed to satisfy detailed balance at temperature T with ferromagnetic coupling ($J>0$) between the spins in order to describe the expected attraction among the C's. Assuming the usual nearest-neighbor Ising Hamiltonian,

$$H=-J\sum_{\langle \mathbf{r},\mathbf{r}'\rangle}\sigma_{\mathbf{r}}\sigma_{\mathbf{r}'}, \tag{6}$$

the rate of exchange between neighboring sites $\mathbf{r}$ and $\mathbf{r}'$ can be chosen to be[29]

$$w_{\mathbf{r}\leftrightarrow\mathbf{r}'}=\frac{1}{\tau_e}[1+e^{\delta E/(k_BT)}]^{-1}, \tag{7}$$

where τ_e sets the time scale, T and k_B are the temperature and the Boltzmann constant, respectively, and δE is the change in the energy $\delta E=\delta H(\sigma_{\mathbf{r}}\leftrightarrow\sigma_{\mathbf{r}'})$ due to the exchange of spins at $\mathbf{r}$ and $\mathbf{r}'$.

Without the spin-flip dynamics, the system would relax to the equilibrium of the Ising model at temperature T and at fixed magnetization. Thus choosing the temperature low enough (below T_c of the Ising model) and making the spin-flip front produce the right magnetization density, the system will be in the unstable part of the phase diagram of the Ising model and phase separation will take place. If this model represents the pattern forming process correctly then one expects the emergence of bands of up and down spins in the wake of the moving spin-flip front.

III. SIMULATION RESULTS

A. Parameters

Monte Carlo simulations of the kinetic Ising model described above have been performed in dimensions $d=2$ and 3. The dimension-specific properties of the lattices used in the simulations will be given in the appropriate subsections below. Here we enumerate and discuss only those adjustable parameters which are used independently of dimension:

(1) The temperature T is measured in units of J/k_B, where J is the nearest-neighbor coupling of the Ising model (6). It is clear from the considerations of the previous section that $T<T_c$ should be used.
(2) The particle concentration, c_0, deposited by the front must be chosen so that, at the given T, it places the system in the metastable or unstable region of the phase diagram of the Ising model.
(3) Length is measured in units of the lattice spacing a. It should be noted that the value of a depends on the interpretation of C and a can be a microscopic length-scale as well as a mesoscopic one.
(4) Time is measured in units of the ''microscopic'' time scale τ_e [see Eq. (7)]. Again, this time scale may be coming from microscopic or mesoscopic processes depending on the interpretation of C.
(5) The diffusion coefficient of the front (D_f) is, in principle, a well defined quantity.[5] The uncertainty of the connection between the microscopic and macroscopic length- and time-scales, however, makes it difficult to set a value for D_f in terms of a and τ_e. We shall thus treat D_f as a parameter that can be freely varied.
(6) The width of the reaction front (2Δ) does not appear to influence the emerging patterns (this is the experience both from the mean-field theory[4] and from small scale simulations). Thus, in most of our simulations, we set $\Delta=1/2$, i.e., the front coincides with one of the lattice planes perpendicular to the motion of the front.

The three important parameters are T, c_0, and D_f, and one should search for pattern formation in this three-dimensional parameter space. This is not necessarily an easy task since it is known, both experimentally[2] and theoretically,[21] that patterns are formed only in a restricted domain of the available free parameters. Since our search is finite, our statements (especially about the absence of patterns) are always pertinent only to the parameter domain investigated.

B. Two-dimensional simulations

Simulations have been performed on stripes of length L_x and width $L_y=50$ or 100 with periodic boundary conditions in the transverse (y) direction. L_x was chosen to be long enough so that no end effects would be observed with $L_x=3000$ being a typical value. The initial position of the front was always at $x=1$ and we used closed boundary conditions (no particle crossing) at both $x=0$ and $x=L_x$.

The possible formation of patterns was investigated for the following ranges of the adjustable parameters, $0.02\leqslant T\leqslant 1.5$, $0.01\leqslant D_f\leqslant 1$, and $0.05\leqslant c_0\leqslant 0.5$. About 200 sets of values have been studied in the above domain and no regular patterns were observed. A typical result is displayed in Fig. 1 for $T=0.7$, $D_f=0.025$, and $c_0=0.3$.

We have also made a few simulations outside of the above domain in order to check the possible strong effect of the changes in a single parameter. These nonsystematic searches did not lead to pattern-forming regimes either.

We have extended the simulations to cases where the interactions are not restricted to nearest neighbors but extend

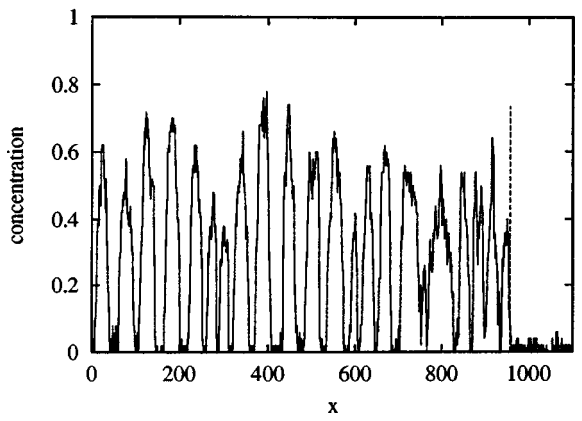

FIG. 1. Concentration profile of C's averaged over the transverse direction for a two-dimensional pattern obtained in a stripe of size 50×3000 with $T=0.7$, $D_f=0.025$, and $c_0=0.3$. The distance along the slab (x) is measured in units of the lattice spacing. The dotted line shows the position of the front at the time ($t=1.8\times10^7$) the concentration was measured. The time is in units of the inverse of the rate of hopping for free C particles (τ_e).

up to seven lattice spacings. No patterns were found, although the randomness of the pattern slightly decreased when the range of the interaction was increased. This is expected as in the limit of long-range interactions one should reach a continuum, noiseless limit. Thus the Cahn–Hilliard description [Eq. (2)] should apply and we should observe regular band formation.

The nonexistence of regular banding should not be considered as a contradiction with the experimental observations of $d=2$ Liesegang patterns. The experimental systems always have macroscopic width in the third dimension and this appears to stabilize the patterns. Indeed, Fig. 2 shows a simulation with the same parameters as those in Fig. 1, except an extra layer in the third dimension is added. As one can see, the bands in the two-layer system are much better defined and they display some regularity. Note in particular, that the concentration within the bands in Fig. 2 has reached the equilibrium value ($c\approx c_p\approx1$) while the maximum concentration regions in Fig. 1 are roughly halfway in between the equilibrium values, $c_g\approx0$ and $c_p\approx1$.

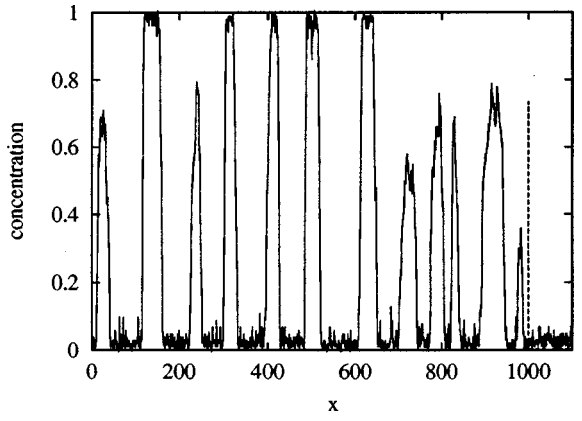

FIG. 2. Concentration pattern in a system of size $50\times2\times3000$. The parameters T, D_f, and c_0 and the notations are the same as on Fig. 1. The dotted line shows the position of the front.

C. Three-dimensional simulations

The simulations were performed on slabs of length L_x and of cross section of size $L_y\times L_z$. Periodic boundary conditions were used in the transverse (y,z) directions while closed boundary conditions were employed at the two ends of the slabs. As in the two-dimensional case, L_x was chosen so ($L_x\approx3000$) as to avoid end effects from the transverse wall at $x=L_x$. Most of the simulations were done for $L_y=L_z\equiv L=10$, 20, and 40 in order to observe finite-size effects. The initial condition was again an empty (all spins down) state with the front situated at $x=1$.

Precipitation patterns were observed for $T\leqslant1$ if $c_0\geqslant0.25$ was chosen well in the metastable or unstable region of the phase diagram of the $d=3$ Ising model. For large front diffusion ($D_f\geqslant1$), these patterns were not regularly spaced and were not stable. Namely, coarsening was observed within reasonable observation time (time of formation of about 7–10 bands). A typical example is shown on Fig. 3.

The bands are more stable at lower temperatures ($T\leqslant0.8$) and their spacing becomes more regular, as the front diffusion coefficient is decreased below $D_f\leqslant0.1$. For $D_f\leqslant0.05$, one observes the emergence of Liesegang-type band patterns, typical examples being those shown on Figs. 4(a)–4(c). In this case, the system is of size ($L\times L\times3000$) and the parameter values used are $T=0.7$, $D_f=0.025$, and $c_0=0.3$. Results of runs for three cross sections ($L=10$, 20, and 40) are displayed. Comparing these pictures, one cannot see any obvious finite-size trends.

In order to investigate the spacing law one would need a large number of bands. Unfortunately, in the regime where the best Liesegang-type patterns are obtained one is restricted in the extent of explorations by the computing resources. Due to the low value of D_f, the front is moving very slowly and consequently the computation time for obtaining, e.g., 10 bands becomes very large. The CPU time necessary to produce the pattern in Fig. 4(a) was about 1500 h on a Sun Ultra-10 workstation.

Figure 4 shows roughly the limits of the possibilities of our simulations at present. To establish the spacing law firmly, we would certainly need more bands. Using the last 4–6 bands obtained from pictures similar to those on Fig. 4, one can see that the positions of the bands (x_n) do approximate a geometric series $x_n\sim(1+p)^n$ well, and one can extract an approximate the spacing parameter, p. In general, we find that the spacing coefficient does not show discernible finite-size trends. For example, the spacing parameter is $p\approx0.17$ for all values of L in Fig. 4.

An interesting feature of the patterns emerging in our simulations is the presence of material (C) in between the bands [see Figs. 3(a)–3(c) and 4(a)–4(c)]. Of course, it is not entirely clear whether part of this material should be considered as a low density precipitate (seen in many experiments[2]) or should it be just regarded as a ''gas'' phase of particles C. Visual inspection of the interband region reveals the presence of both small clusters and single particles. The small clusters live long (especially at lower temperatures), their lifetime is comparable to the time of formation of several bands. Thus the interpretation of part of the interband material as low density precipitate may have some validity. In

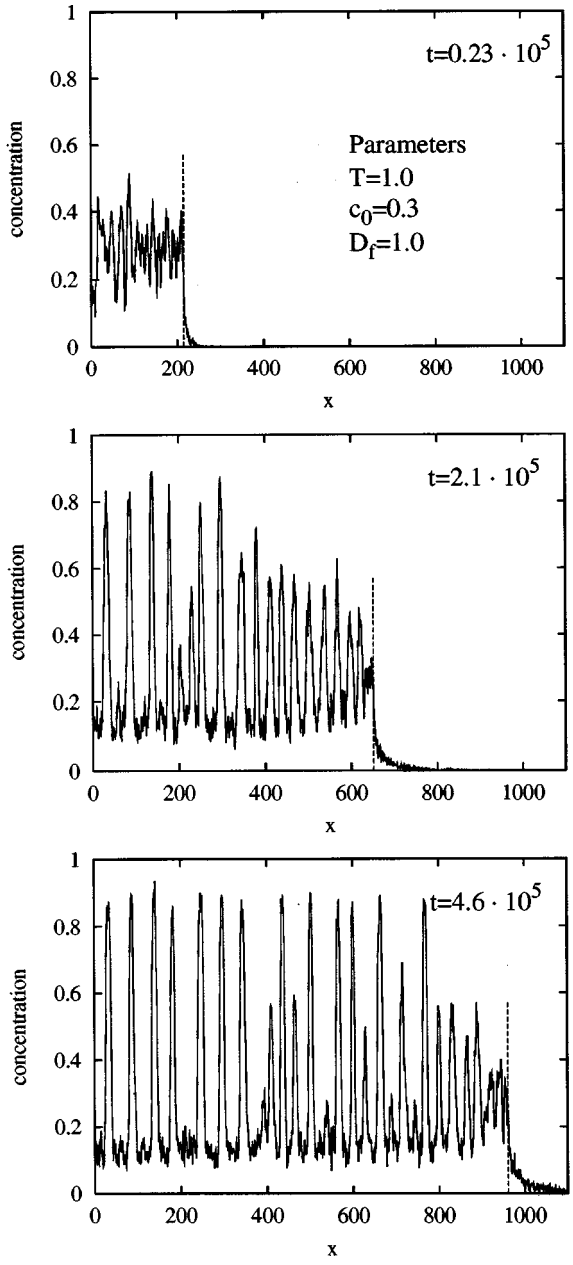

FIG. 3. Time evolution of the concentration of C particles averaged over the transverse (y,z) directions in slabs of size $20\times20\times3000$. The parameters ($T=1.0$, $D_f=1.0$, $c_0=0.4$) were chosen to be in the ''coarsening pattern'' regime. The time is given in units of τ_e that is the inverse of the rate of hopping for free C particles. The distance along the slab (x) is measured in units of the lattice spacing. The dotted lines show the positions of the reaction front at time t.

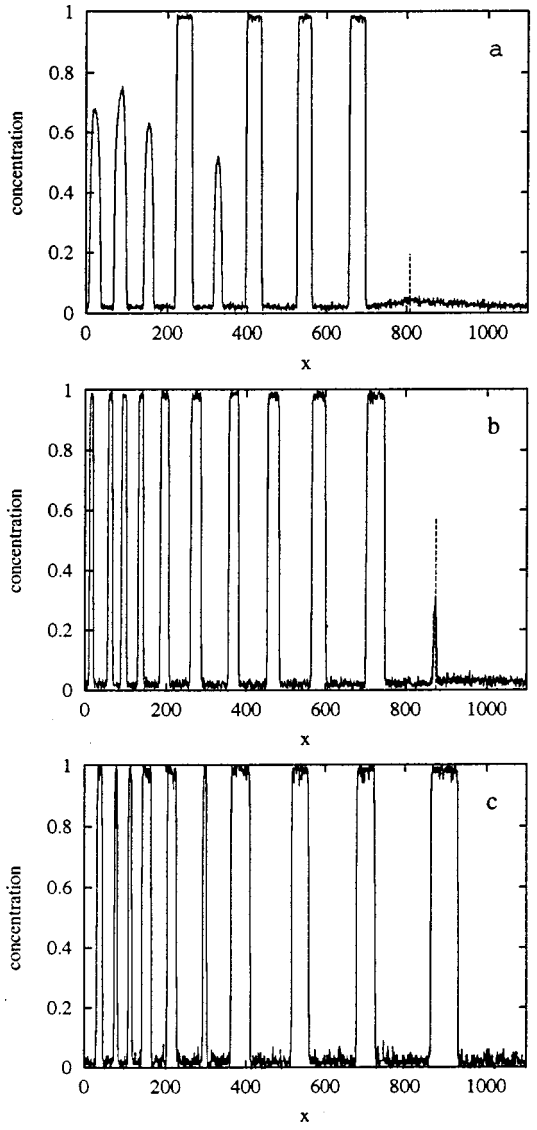

FIG. 4. Concentration averaged over the transverse (y,z) directions in slabs of size $L\times L\times3000$. The values of the parameters ($T=0.7$, $D_f=0.025$, and $c_0=0.3$) are the same for three transverse sizes $L=40$ (a), $L=20$ (b), and $L=10$ (c). The distance along the slab (x) is measured in units of the lattice spacing. The dotted lines show the positions of the reaction front [the front is off the scale on Fig. 4(c)].

order to make progress in this problem, one would need larger scale simulations as well as more understanding of the connection between the microscopic and macroscopic time- and length-scales.

IV. FINAL REMARKS

Apart from the simplicity, an important feature of our model is that fluctuations are included. A frequent consequence of the presence of fluctuations is the disappearance of order in low dimensions and, indeed, our simulations also indicate that Liesegang type patterns are absent in $d=2$ dimension while they exist in $d=3$ dimensional samples.

Another advantage of including the noise is that the model has pattern-forming regimes which have characteristics of either the prenucleation theories[20,21] or the postnucleation competitive growth theories.[22] Indeed, one can see [Fig. 4(b)] that the bands are forming at the position of the reaction front for D_f small, while the bands are formed as a result of coarsening and competitive growth well behind the front in case of large D_f (Fig. 3). Note that the absence of Liesegang-type patterns in the second regime is in agreement with the inability of producing such patterns in postnuclation competitive growth theories.[22]

We feel that the most important feature of the model is that it makes clear that the important and experimentally controllable parameters are T, c_0, and D_f. Indeed, both c_0

and D_f are known functions of the initial densities (a_0,b_0) and diffusion constants $(D=D_a\approx D_b)$ of reagents A and B the $A+B\rightarrow C$ reaction.[5,24,25] Although the diffusion constants D_a and D_b are usually not controllable, a_0 and b_0 can be set to given values and, consequently, c_0 and D_f can be varied independently.

Among the three parameters, a change in T leads to unpredictable changes in the various diffusion coefficients and background processes in a real Liesegang experiment (for example, the diffusion coefficients of the background ions may also be important[30] in determining the spacing coefficient). Thus it is advisable to keep the temperature constant, and the most promising and, indeed, most often used way of looking for trends in experiments[8,9] is the change of the concentrations of the inner and outer electrolytes (a_0 and b_0).

An obvious consequence of our simulations is that one should be able to observe a crossover from prenucleation regime to a regime where postnucleation processes are dominant. Namely this could be achieved by tuning a_0 and b_0 in such a way that, at fixed c_0, the front diffusion coefficient D_f would be varied over as much a range as possible.

In closing, let us discuss the possible connection between the parameters in the kinetic Ising model and in the Cahn–Hilliard equation. There is a long history of trying to derive hydrodynamical equations (such as the Cahn–Hilliard equation) from kinetic Ising models[31–36] by taking a naive continuum limit. These works have been most important in identifying Langevin equations of correct symmetry in the continuum limit but, in general, they have not been useful for deriving macroscopic parameter values. The reason for the failure is quite clear. On the way from microscopics to macroscopics, one changes the length-scale by several order of magnitudes and one must average over the the microscopic degrees of freedom. This averaging renormalizes the parameters but, in taking the naive continuum limit, the averaging is not carried out or carried out in a highly simplified and uncontrolled manner. Thus, a meaningful comparison of the Cahn–Hilliard and the kinetic Ising model description of the Liesegang phenomena is a nontrivial matter and it has not been dealt with in this paper.

We note, however, that there may be a phenomenological (''experimental'') way to do the comparison. Namely, one can investigate the various patterns produced by the two models in the various regions of the parameter space and make a fit of matching parameter values by searching for matching patterns. The problem with this type of approach is that, at present, the production of patterns by the kinetic Ising model is limited to a few bands (see Fig. 4) due to limited computer power. One expects, however, that the available computer power will be soon sufficient to carry out the above project.

ACKNOWLEDGMENTS

This work has been supported by the Swiss National Science Foundation and by the Hungarian Academy of Sciences (Grant No. OTKA T 029792).

[1] R. E. Liesegang, Naturwiss. Wochenschr. **11**, 353 (1896).
[2] H. K. Henisch, *Periodic Precipitation* (Pergamon, Oxford, 1991).
[3] For a recent comparison between theories and experiments, see T. Antal, M. Droz, J. Magnin Z. Rácz, and M. Zriny, J. Chem. Phys. **109**, 9479 (1998).
[4] T. Antal, M. Droz, J. Magnin, and Z. Rácz, Phys. Rev. Lett. **83**, 2880 (1999).
[5] L. Gálfi and Z. Rácz, Phys. Rev. A **38**, 3151 (1988).
[6] J. W. Cahn and J. E. Hilliard, J. Chem. Phys. **28**, 258 (1958); J. W. Cahn, Acta Metall. **9**, 795 (1961).
[7] K. Jablczynski, Bull. Soc. Chim. Fr. **33**, 1592 (1923).
[8] R. Matalon and A. Packter, J. Colloid Sci. **10**, 46 (1955).
[9] A. Packter, Kolloid-Z. **142**, 109 (1955).
[10] Z. Rácz, Physica A **274**, 50 (1999).
[11] J. Magnin, Ph.D. thesis, University of Geneva, 2000.
[12] S. C. Müller, S. Kai, and J. Ross, J. Phys. Chem. **86**, 4078 (1982); B. Chopard, M. Droz, J. Magnin, and M. Zrinyi, J. Chem. Phys. **110**, 9618 (1999).
[13] P. C. Hohenberg and B. I. Halperin, Rev. Mod. Phys. **49**, 435 (1977).
[14] S. Cornell and M. Droz, Phys. Rev. Lett. **70**, 3824 (1993).
[15] Up to a few years ago, the smallest distances between bands achieved in experiments were of the order of $\lambda\approx 10\mu$. Recent reports show a decrease of λ to $\lambda\approx 1\mu$ [X. G. Zheng, M. Taira, M. Suzuki, and C. N. Xu, Appl. Phys. Lett. **72**, 1155 (1998); P. Hantz, ''Pattern formation in reaction-diffusion systems,'' thesis, Eötvös University, Budapest, 1998].
[16] W. Ostwald, *Lehrbuch der Allgemeinen Chemie* (Engelman, Leipzig, 1897).
[17] C. Wagner, J. Colloid Sci. **5**, 85 (1950); S. Prager, J. Chem. Phys. **25**, 279 (1956); Ya. B. Zeldovitch, G. I. Barrenblatt, and R. L. Salganik, Sov. Phys. Dokl. **6**, 869 (1962). In these theories the reactants turn directly into precipitate ($A+B\rightarrow D$) thus the dynamics of the intermediate product C does not arise.
[18] N. R. Dhar and A. C. Chatterji, Kolloid-Z. **37**, 2 (1925); J. Phys. Chem. **28**, 41 (1924).
[19] S. Shinohara, J. Phys. Soc. Jpn. **29**, 1073 (1970).
[20] G. T. Dee, Phys. Rev. Lett. **57**, 275 (1986).
[21] B. Chopard, P. Luthi, and M. Droz, Phys. Rev. Lett. **72**, 1384 (1994); J. Stat. Phys. **76**, 661 (1994).
[22] M. Flicker and J. Ross, J. Chem. Phys. **60**, 3458 (1974); S. Kai, S. C. Müller, and J. Ross, *ibid.* **76**, 1392 (1982); R. Feeney, S. L. Schmidt, P. Strickholm, J. Chadam, and P. Ortoleva, *ibid.* **78**, 1293 (1983); G. Venzl, *ibid.* **85**, 1996 (1986); **85**, 2006 (1986). These works attribute the Liesegang band formation to the instability present in the postnucleation coarsening process. They cannot explain, however, the regular aspects of the band spacing.
[23] M. Chacron and I. L'Heureux, Phys. Lett. A **263**, 70 (1999); I. L'Heureux, Phys. Rev. E **62**, 3234 (2000). This is an attempt to make a synthesis of pre- and postnucleation theories. No quantitative analysis of the resulting patterns were carried out.
[24] The case of unequal diffusion coefficients is treated in Z. Koza, J. Stat. Phys. **85**, 179 (1996).
[25] More complicated reaction schemes ($A+2B\rightarrow C$ and $2A+B\rightarrow C$) are studied in J. Magnin, Eur. Phys. J. B **17**, 673 (2000).
[26] M. Droz, Z. Rácz, and J. Schmidt, Phys. Rev. A **39**, 2141 (1989).
[27] R. J. Glauber, J. Math. Phys. **4**, 294 (1963).
[28] H. Larralde, M. Araujo, S. Havlin, and H. E. Stanley, Phys. Rev. A **46**, 855 (1992).
[29] K. Kawasaki, Phys. Rev. **145**, 224 (1966).
[30] T. Unger and Z. Rácz, Phys. Rev. E **61**, 3583 (2000).
[31] M. Plischke, Z. Rácz, and D. Liu, Phys. Rev. B **35**, 3485 (1987).
[32] Z. Rácz, M. Siegert, D. Liu, and M. Plischke, Phys. Rev. A **43**, 5275 (1991).
[33] K. Binder and H. L. Frisch, Z. Phys. B: Condens. Matter **84**, 403 (1991).
[34] D. D. Vvedensk, A. Zangwill, C. N. Luse, and R. M. Wilby, Phys. Rev. E **48**, 852 (1993).
[35] M. Predota and M. Kotrla, Phys. Rev. E **54**, 3933 (1996).
[36] K. Leung, cond-mat/0006217.